Fast and robust quantum state transfer in a topological Su-Schrieffer-Heeger chain with Next-to-Nearest-Neighbour interactions

Felippo M. D'Angelis[1], Felipe A. Pinheiro[1], David Guéry-Odelin[2], Stefano Longhi[3,4], François Impens[1]
[1] *Instituto de Física, Universidade Federal do Rio de Janeiro, Rio de Janeiro, RJ 21941-972, Brazil*
[2] *Laboratoire Collisions, Agrégats, Réactivité, IRSAMC, Université de Toulouse, CNRS, UPS, France*
[3] *Dipartimento di Fisica, Politecnico di Milano, Piazza L. da Vinci 32, I-20133 Milano, Italy*
[4] *IFISC (UIB-CSIC), Instituto de Fisica Interdisciplinar y Sistemas Complejos, Palma de Mallorca, E-07122. Spain*
(Dated: June 18, 2020)

We suggest a method for fast and robust quantum-state transfer in a Su-Schrieffer-Heeger (SSH) chain, which exploits the use of next-to-nearest-neighbour (NNN) interactions. The proposed quantum protocol combines a rapid change in one of the topological edge states, induced by a modulation of nearest-neighbour interactions, with a fine tuning of NNN interactions operating a counter-adiabatic driving. The latter cancels nonadiabatic excitations from the edge state multiplicity to the energy bands. We use this shortcut technique for topological pumping of edge states on a single dimerized chain and also through an interface that connects two dimerized Su-Schrieffer-Heeger chains with different topological order. We investigate the robustness of this protocol against both uncorrelated and correlated disorder, and demonstrate its strong resilience to the former in comparison to traditional adiabatic protocols for topological chains. We show that introducing spatial correlations in the disorder increases the robustness of the protocol, widening the range of its applicability.

I. INTRODUCTION

A promising route to develop quantum information architectures, resilient against decoherence, is to implement the operation on a subset of quantum states that benefit from a natural protection – for instance when they belong to a specific symmetry class which is immune to decoherence [1]. The robustness of topological protection [2] has turned topological quantum systems into excellent candidates of quantum computing platforms [3], which has motivated their implementation in either photonic [4–7] or atomic systems [8]. In order to obtain universal quantum computation, such architectures must be able to perform a finite set of elementary tasks with a high degree of reliability, among which local operations on single qubits, generation of entangled states, and quantum states transfer within the quantum register [3].

In this work, we put forward a fast and resilient protocol for quantum state transfer in a Su-Schrieffer-Heeger (SSH) chain [9], which provides the simplest one-dimensional lattice with topologically-protected edge states. Among relevant previous examples of transfer protocols, we mention the use of time-independent fields in coupled quantum dots [10], protocols relying on single-qubit Rabi flopping protocols [3, 11, 12], the transfer of doublons across a spin chain [13], and Thouless pumping [4, 5]. A strong motivation to develop quantum computation on a topological register is the intrinsic resilience against stochastic perturbations. In this line, a key feature of toplogical quantum state transfer protocols should be to preserve this robustness, and to be resilient against possible imperfections in the dynamical control parameters as well as against local and long-range parasitic fluctuations affecting the spin chain. For this purpose, adiabatic protocols have been considered in a topological spin chain, based on the use of Landau-Zener (LZ) [14] or Stimulated Raman Adiabatic Passage (STIRAP) [15] on a subset of edge states isolated from the continuum. These procedures have shown a good resilience against uncorrelated disorder, but their speed is intrinsically limited by the adiabaticity requirement - both to avoid unwanted nonadiabatic transition within the edge-state multiplicity, and from the edge-state multiplicity to the energy bands. Fast quantum state transfer is also a desirable feature to limit the impact of decoherence. Thus, the application of shortcut-to-adiabaticity techniques [16], suggested to accelerate state transfer protocols in topologically-trivial systems [17–21], seems suitable in the context of topological chains. Initial steps have been taken in this direction [22, 23], with few experimental realizations so far [24, 25].

Here, we present an accelerated protocol of high performance on both a single SSH chain and a succession of two SSH chains having distinct topological orders. Our method is extremely robust against disorder, both uncorrelated and correlated, and even outperforms adiabatic protocols in this respect. Our approach is based on an engineering of Next-to-Nearest Neighbor(NNN) interactions between the sites of the chain, which exactly cancels the excitations towards the band even for a strongly accelerated transfer.

The paper is organized as follows. In Section II, we present the procedure and illustrate the method on a single SSH chain. In Section III, we apply our method to a SSH chain with two distinct topologies and obtain a fast quantum state transfer across the topological interface. In Section IV, we investigate numerically the resilience of the excitation transfer protocol to disorder, considering on-site (diagonal) static disorder in the chain –either uncorrelated or correlated disorder–and fluctuations of the driving NNN interaction strengths. Finally, the main conclusions are outlined in Sec.V.

II. PRINCIPLE OF THE NEXT-TO-NEAREST-NEIGHBOUR INTERACTION ASSISTED TRANSFER

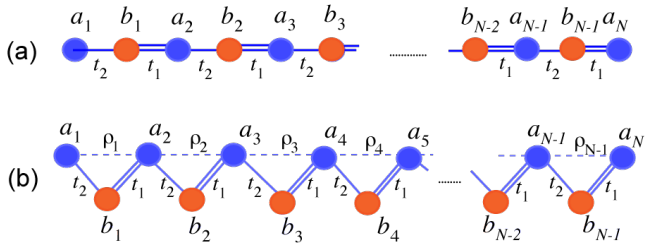

FIG. 1: Diagram showing the SSH chain with (a) nearest neighbour hopping and (b) additional next-to-nearest neighbour hopping (dashed line).

A standard model of quantum state transfer exploiting topological edge states is provided by a SSH chain formed by two sub-lattices with chiral symmetry [3, 12, 14, 26]. Several experimental platforms have already enabled the emulation of SSH chains: in nanophotonics with polaritons in an array of micropillars [6], in granular chains [27], in a 1D bichromatic lattice [28], in arrays of optically trapped Rydberg atoms [8] or in a momentum-space lattice [29].

To exemplify our method, we consider in this section a single chain that contains respectively N sites in the sublattice A and $N-1$ sites in the sublattice B, with alternate nearest-neighbour (NN) time-dependent hopping amplitudes $t_1(t)$ and $t_2(t)$ (see Fig. 1a). This latter requirement can be experimentally implemented. For instance, in Ref. [29], the effective tunneling transition are field driven and as such can be readily made time-dependent.

In the basis of Wannier states and in the single excitation sector, this quantum system is described by the SSH Hamiltonian

$$\hat{H}_0(t) = \sum_{n=1}^{N-1} \Big(t_2(t)|B_n\rangle\langle A_n| + t_1(t)|A_{n+1}\rangle\langle B_n| \Big) + \text{h.c.} \tag{1}$$

The quantum state of the chain is represented by a $2N-1$ state vector $|\psi(t)\rangle$. For an odd number of sites, the SSH Hamiltonian has a single zero-energy mode lying in the gap separating the two energy bands, and localized at the left edge of the chain for $t_2 \ll t_1$:

$$|\phi_0\rangle = \mathcal{N} \sum_{n=1}^{N} \left(\frac{-t_2}{t_1} \right)^{n-1} |A_n\rangle \tag{2}$$

This zero-energy mode is parametrized according to $\epsilon = -t_2/t_1$, which determines the normalization constant $\mathcal{N} = [(\epsilon^2-1)/(\epsilon^{2N}-1)]^{1/2}$. At $t_1 = t_2$, i.e. at the band closing point, this state is fully delocalized along the chain. Finally, for $t_2 \gg t_1$, the eigenstate $|\phi_0\rangle$ is localized at the right end of the chain. Let us assume that the state vector is initially at the left chain boundary, taking for instance $|\psi(0)\rangle = |A_1\rangle$. A full transfer to the right end of the chain amounts to obtaining $|\langle A_N|\psi(T)\rangle|^2 = 1$ at the final time T of the protocol. By slowly changing the time-dependent hopping parameters $t_1(t)$ and $t_2(t)$ so that $\epsilon(t)$ evolve from $\epsilon(t=0) \ll 1$ to $\epsilon(t=T) \gg 1$, one can induce such a transfer by an adiabatic evolution of the instantaneous Hamiltonian eigenstate $|\phi_0(t)\rangle$. However, in order to prevent nonadiabatic transitions to the continuum of states, according to the adiabatic theorem this strategy requires –roughly speaking- that the temporal variation of the hopping terms be much slower than the energy gap between the edge mode and the band. Since in the adiabatic evolution the gap closes at the time for which $t_1 = t_2$, nonadiabatic effects might provide a severe limitation to the quantum state transfer efficiency. Here we unveil a powerful means to overcome the adiabaticity constraint with a dynamical control of NNN interactions inspired by counter-diabatic driving methods. We assume from now on that the SSH chain is dressed by NNN couplings which can be controlled dynamically, as shown in Fig. 1(b). The quantum chain is thus governed by the following Hamiltonian

$$\hat{H}(t) = \hat{H}_0(t) + \sum_{n=1}^{N-1} \Big(i\rho_n(t)|A_{n+1}\rangle\langle A_n| + \text{H.c.} \Big) \tag{3}$$

The NNN hopping amplitudes ρ_m are assumed real-valued. We will justify hereafter the $\pi/2$ dephasing factor between NN and NNN couplings. The purpose of the time-dependent NNN hoppings $\rho_m(t)$ is to cancel exactly non-adiabatic transitions from the time-dependent eigenvector $|\phi_0(t)\rangle$. Differently from the traditional counter-adiabatic driving method [30] that prevent non-adiabatic transitions from all instantaneous eigenstates, our approach cancels only the adiabatic transitions from the topological mode $|\phi_0(t)\rangle$, which is sufficient to achieve a reliable transfer. This trick considerably simplifies the form of the driving terms, enabling one to implement the method with only NNN interactions in one of the sublattices.

From the Schrödinger equation with $\hbar = 1$ associated to Eq. (3), we get the following set of coupled equations that describe the time evolution of the amplitude probabilities $a_n(t)$ and $b_n(t)$ in each sublattice:

$$i\frac{\mathrm{d}a_n}{\mathrm{d}t} = t_2 b_n + t_1 b_{n-1} - i\rho_n a_{n+1} + i\rho_{n-1} a_{n-1}, \tag{4}$$

$$i\frac{\mathrm{d}b_n}{\mathrm{d}t} = t_2 a_n + t_1 a_{n+1}, \tag{5}$$

with $2 \le n \le N-2$ and where explicit time-dependence have been omitted to simplify notations. The amplitude probabilities associated to the chain boundaries satisfy

the specific equations:

$$i\frac{\mathrm{d}a_1}{\mathrm{d}t} = t_2 b_1 - i\rho_1 a_2, \tag{6}$$

$$i\frac{\mathrm{d}a_N}{\mathrm{d}t} = t_1 b_{N-1} + i\rho_{N-1} a_{N-1}. \tag{7}$$

Our goal is to inverse-engineer these equations for a given time-dependence of the NN hopping terms $t_{1,2}(t)$ such that the time-dependent $|\phi_0(t)\rangle$ state, defined by Eq.(2), is an *exact* solution to the time-dependent Schrödinger equation. To determine the profiles of the NNN hopping amplitudes $\rho_n(t)$, let us first notice that, as this state vector has no overlap with "B" sites, one has $b_n(t) = 0$ for $n = 1, ..., N-1$. Furthermore, the form of the wave-vector $|\phi_0(t)\rangle$ guarantees that Eqs.(5) are fulfilled by construction for $b_n(t) = 0$, independently of the specific choices for the hopping amplitudes $t_{1,2}(t)$ and $\rho_n(t)$. Incidentally, this makes the protocol immune to the eventual presence of additional parasitic NNN couplings between the "B" sites. Equation (6) determines $\rho_1(t)$, while Eqs. (4) fix the remaining NNN hoping terms $\rho_n(t)$ for $n = 2, ..., N-1$. Preservation of the norm of the quantum state vector guarantees that Eq. (7) is fulfilled. The wave-vector $|L(t)\rangle$ evolves indeed on a manifold of dimension $N-1$, so that any quantum trajectory associated to a unitary evolution can be obtained with an appropriate parametrization of the $N-1$ hopping amplitudes $\rho_n(t)$. From Eqs.(4) and (6), one ends up with the following set of recurrence relations:

$$\rho_1 = -\frac{1}{a_2}\frac{\mathrm{d}a_1}{\mathrm{d}t}, \tag{8}$$

$$\rho_n = \frac{1}{\epsilon^2}\rho_{n-1} - \frac{(n-1)\hbar}{\epsilon^2}\frac{\mathrm{d}\epsilon}{\mathrm{d}t} - \frac{1}{\epsilon}\frac{\mathrm{d}\ln(\mathcal{N})}{\mathrm{d}t}, \tag{9}$$

with $2 \leq n \leq N-1$.

It is instructive to consider the quantum-state transfer in a 3-sites chain, which corresponds to the well-known STIRAP scheme. In this case our method reduces to the counterdiabatic driving method [31], involving a single coupling $\rho_1(t)$. The Schrödinger equation yields a simple three-equation system for the amplitudes $a_1(t)$, $b_2(t)$ and $a_2(t)$. The relevant adiabatic zero-energy mode is given by $a_n = \epsilon^{n-1}/\sqrt{1+\epsilon^2}$ for $n = 1, 2$ and the recurrence relation (8) yields the NNN coupling $\rho_1(t) = (1+\epsilon^2)^{-1}\frac{\mathrm{d}\epsilon}{\mathrm{d}t}$. Hopping amplitudes $t_1(t), t_2(t)$ must fulfil the boundary conditions $|t_1(0)/t_2(0)| \ll 1$ and $|t_1(T)/t_2(T)| \gg 1$ required to achieve a high fidelity in the quantum state transfer. There is an infinity of possible choices, and one may privilege a particular profile depending on the feasibility of the experimental implementation. By taking for instance a sinusoidal modulation of the NN couplings $t_1(t) = t_0\cos[\pi t/(2T)]$ and $t_2(t) = t_0\sin[\pi t/(2T)]$ with t_0 an arbitrary constant energy, one finds a particularly simple, constant counter-driving term $\rho_1(t) = -\pi/2T$. As expected, this counter-adiabatic coupling vanishes in the adiabatic limit. The expression of the NNN hopping terms $\rho_n(t)$ becomes increasingly intricate as we consider longer chains.

To illustrate the validity of our procedure when considering longer chains, we apply the method to a SSH chain of $2N-1 = 19$ atoms in the configuration depicted in Fig 1(b) for a total duration $T = 2/t_0$, where t_0 is the largest value taken by the hopping amplitude t_1 (or t_2) in the transfer process. Clearly, such a short time transfer violates the adiabaticity criterion and, without counter-diabatic driving, the transfer efficiency is greatly degraded (less than 1 %). In order to speed-up numerical calculations, and similarly to many shortcut-to-adiabaticity protocols [16, 32–34], we have parametrized the quantum state trajectory with polynomial – the simplest functions to fulfill the required set of boundary conditions. Precisely, we have taken NN hoppings $t_1(t) = t_0 P(t/T)$ and $t_2(t) = t_0(1 - P(t/T))$ with the polynomial $P(x) = 2x^3 - 3x^2 + 1$. $P(x)$ is indeed the lowest order polynomial fulfilling the conditions $P(0) = 1$, $P(1) = 0$ together with a cancellation of the derivatives at the boundary of the time interval. The latter is necessary to ensure a smooth parabolic switching on/off of the NN hoppings. The corresponding results, depicted in Fig.2, have been obtained from a full numerical resolution of the Schrödinger equation in the presence of the time-dependent NN and NNN interactions. They confirm the consistency of our approach, i.e. that a perfect transfer is achieved thanks to the counter-diabatic driving with NNN interactions. Figure 3 shows the time-dependence of the NNN coefficients $\rho_n(t)$ along the chain. Symmetry considerations show that $\rho_{N-1-n}(t) = \rho_n(T-t)$, so that we only represent the couplings $\rho_n(t)$ for $k = 1, ..., \lceil N/2 \rceil$.

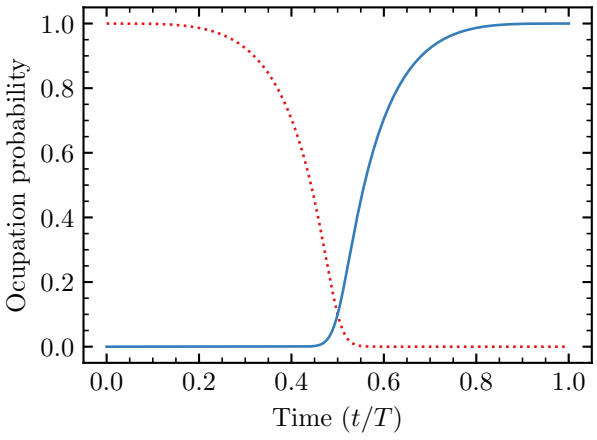

FIG. 2: Time-dependent probability of occupation of the sites A_1 (red-dotted line) and A_N (blue solid line) in a SSH chain with NNN-assisted coupling. The chain comprises $N = 10$ sites in sublattice A. NN hopping amplitudes used in the numerical simulations are $t_1(t) = t_0 P(t/T)$ and $t_2(t) = t_0[1 - P(t/T)]$ with the polynomial $P(x) = 2x^3 - 3x^2 + 1$ and with a total transfer time $T = 2/t_0$.

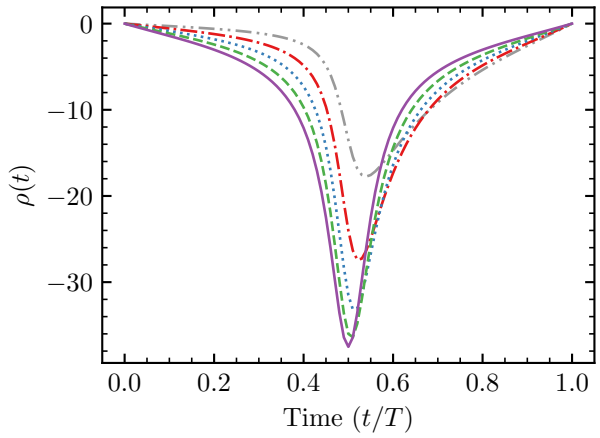

FIG. 3: Profile of the NNN couplings $\rho_n(t)$ (in units of t_0) as prescribed by the NNN-interaction assisted transfer for $n = 1, .., 5$ (dash-dot-dotted gray, dash-dotted red, dotted blue, dashed green and solid purple lines respectively). Parameter values are as in Fig.2.

III. NEXT-TO-NEAREST-NEIGHBOUR-INTERACTION-ASSISTED TRANSFER ACROSS A TOPOLOGICAL INTERFACE

We now extend the NNN interaction protocol in order to obtain a fast quantum state transfer across a topological interface. We consider a SSH chain of $4N-1$ atoms involving two fragments of different topologies as represented in Fig. 4. The single excitation sector Hamiltonian

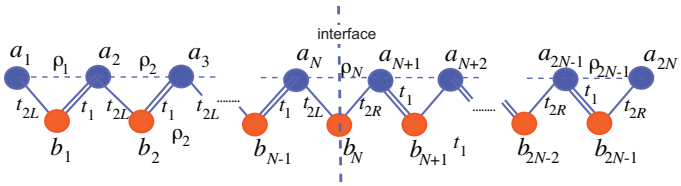

FIG. 4: SSH chain with a topological interface, dressed with dynamically controlled NNN interactions.

now reads:

$$\hat{H}_1(t) = t_{2L}(t)\sum_{n=1}^{N} |B_n\rangle\langle A_n| + t_1(t)\sum_{n=1}^{N-1} |A_{n+1}\rangle\langle B_n| + \text{h.c.} \quad (10)$$

The topology on each side of the interface depends on the parameters $\epsilon_L = -t_{2L}/t_1$ and $\epsilon_R = -t_{2R}/t_1$. When $|\epsilon_L|$ and $|\epsilon_R|$ are both greater than unity, or both smaller than unity, the sides of the chain have different topologies, and the chain exhibits a topological interface at the site b_N. From now on, we consider specifically the regime for which $0 < |\epsilon_L| < 1$ and $0 < |\epsilon_R| < 1$. In this case the chain has three topological modes isolated from the energy bands. In the limit $\epsilon_{L,R} \ll 1$, two of these modes are localized at the chain boundaries, while the third zero-energy mode lies in the vicinity of the interface. A procedure for a quantum state transfer across such a topological SSH chain has been proposed in Ref. [15]. This approach relies on a STIRAP protocol within the 3-state multiplicity of topological states. A dark state, built up from a superposition of two edge states, is then evolved adiabatically from one extremity of the chain to the other. This evolution is obtained by a variation of the hopping amplitudes $t_{2\,L,R}(t)$. Although efficient in the adiabatic limit, the bottleneck of this method is the minimum transfer duration imposed by the adiabaticity condition, which rapidly grows with the chain length.

Following the strategy exposed in the previous Sections, we set up an appropriate engineering of NNN interactions to go beyond this limitation. We prescribe a trajectory along the following zero-energy mode:

$$|\psi_0\rangle = \frac{1}{\mathcal{N}} \begin{pmatrix} \epsilon_R^N \\ 0 \\ \epsilon_L\epsilon_R^N \\ 0 \\ \dots \\ 0 \\ \epsilon_L^{N-1}\epsilon_R^N \\ 0 \\ -\epsilon_L^N\epsilon_R^{N-1} \\ 0 \\ -\epsilon_L^N\epsilon_R^{N-2} \\ 0 \\ \dots \\ 0 \\ -\epsilon_L^N\epsilon_R \\ 0 \\ -\epsilon_L^N \end{pmatrix} \quad (11)$$

where we assume from now on $\epsilon_{L,R} \neq 0$. As previously, this wave-vector is restricted to the sublattice A (odd components). The wave-vector components in the immediate vicinity of the interface are $a_N = \epsilon_L^{N-1}\epsilon_R^N$ and $a_{N+1} = -\epsilon_L^N\epsilon_R^{N-1}$. The time dependence of the parameters ϵ_L, ϵ_R has been omitted to simplify notations. $\mathcal{N}$ is a normalization constant setting the norm of the wave-vector to unity, which can be expressed as $\mathcal{N} = \left[\epsilon_R^{2N}(1-\epsilon_L^{2N})/(1-\epsilon_L^2) + \epsilon_L^{2N}(1-\epsilon_R^{2N})/(1-\epsilon_R^2)\right]^{1/2}$ if $\epsilon_{L,R} \neq 1$.

The prescribed quantum state $|\psi_0(t)\rangle$, given by (11), fulfills, by construction, the projection of the Schrödinger equation on the sublattice B for any time-dependent NN hoppings. In contrast, this wave-vector only satisfies the Schrödinger equation on the sublattice A if appropriate NNN couplings $\rho_n(t)$ are applied. The Hamiltonian including these NNN couplings reads $\hat{H}(t) = \hat{H}_1(t) + \left(\sum_{n=1}^{2N-1} i\rho_n(t)|A_{n+1}\rangle\langle A_n| + \text{H.c}\right)$. The NNN couplings are obtained by an inverse engineering of the Schrödinger

equation. One obtains the following recurrence relations:

$$\begin{aligned}
\rho_1 &= -\frac{1}{\epsilon_L}\frac{\dot{a}_1}{a_1}, \\
\rho_{m+1} &= \frac{\rho_m}{\epsilon_L^2} - m\frac{\dot{\epsilon}_L}{\epsilon_L^2} + \rho_1, \\
\rho_N &= -\frac{\epsilon_R}{\epsilon_L^2}\rho_{N-1} + (N-1)\frac{\epsilon_R\dot{\epsilon}_L}{\epsilon_L^2} + \frac{\epsilon_R}{\epsilon_L}\frac{\dot{a}_1}{a_1}, \\
\rho_{N+1} &= -\frac{\epsilon_R^2}{\epsilon_L^2}\rho_N - N\frac{\epsilon_R\dot{\epsilon}_L}{\epsilon_L} - \epsilon_R\frac{\dot{a}_1}{a_1}, \\
\rho_{n+1} &= \epsilon_R^2\rho_n - N\frac{\epsilon_R\dot{\epsilon}_L}{\epsilon_L} + (n-N)\dot{\epsilon}_R - \dot{\epsilon}_R\frac{\dot{a}_1}{a_1},
\end{aligned} \tag{12}$$

where the m and n indices belong to the intervals $1 \leq m \leq N-2$ and $N+1 \leq n \leq 2N-2$ and with the first wave-vector component $a_1 = \mathcal{N}^{-1}\epsilon_R^N$. Note that the couplings in the immediate vicinity of the interface satisfy different equations. One has again $2N$ equations to be satisfied by $2N-1$ independent parameters $\rho_n(t)$. Thanks to the conservation of the wave-vector norm, this system is not overdetermined.

The choice of the hopping amplitudes $t_1(t)$, $t_{2L}(t)$ and $t_{2R}(t)$ must be compatible with a transfer of the wave-vector (11) from the left to the right boundary of the chain. The initial location at the left end is achieved if $|\epsilon_L(0)| \ll 1$ and a finite value of $|\epsilon_R(0)| < 1$, while the location at the right end is obtained at the final time T if $|\epsilon_R(T)| \ll 1$ with a finite $|\epsilon_L(T)| < 1$. From now on, we simply set $t_1(t) = t_0$ and take for the hopping amplitudes: $t_{2L}(t) = t_0 f(2t/T)$ for $t < T/2$, $t_{2L}(t) = t_0 f(T/2)$ for $t \geq T/2$, and $t_{2R}(t) = t_{2L}(T-t)$. $f(x)$ is a polynomial defined as $f(x) = \delta + (1-2\delta)(3x^2 - 2x^3)$, with $\delta = 0.01$, and the corresponding amplitudes are depicted on Fig. 5(a). By inspection of Eq. (11), this choice provides initial and final locations at the left and right extremities of the chain respectively. One also notes that $0 < |\epsilon_L(t)| < 1$ and $0 < |\epsilon_R(t)| < 1$ at any time, so that the chain maintains a topological interface through the whole process. At the half time $t = T/2$, one has $\epsilon_L(T/2) = \epsilon_R(T/2) = 0.99$, corresponding to a state delocalized on the whole chain for the considered values of N.

The set of recurrence relations (13) may induce NNN coupling amplitudes ρ_n scaling exponentially with n, or even divergent coupling strength for specific times. This would be a serious drawback, as the implementation of such couplings would then require an unrealistic amount of energy in long topological chains. A suitable profile for the NN hoppings should thus yield counterdiabatic driving terms of finite amplitude. As shown in Fig. 5(b), our choice of hopping amplitudes $t_{2L,R}(t)$ yields smooth and well-behaved NNN couplings $\rho_n(t)$. Remarkably, these NNN couplings vanish at the half time $T/2$, when the state is most delocalized along the chain. Figure 5(c) displays the temporal profile of the occupation probabilites associated to the chain boundaries for a total time $T = 40/t_0$. As a consistency check, one notes that a perfect population transfer is obtained at the final time.

IV. RESILIENCE OF THE TRANSFER PROTOCOL AGAINST CORRELATED/UNCORRELATED DISORDER

Any realistic implementation of the protocol will involve a finite amount of disorder, either in the control field operating the NNN couplings, either in the realization of the SSH chain itself. We thus discuss here the resilience of the counter-diabatic protocol to a simplification of its execution, and to the presence of disorder in the realization of the protocol or in the implementation of the SSH chain. The presence of stochastic fluctuations, either in the eigenenergies or in nondiagonal couplings, may decrease the efficiency of the quantum state transfer. Nevertheless, the NNN-interaction assisted transfer presents a surprising resilience against both correlated and uncorrelated disorder, outperforming in this respect previous schemes using adiabatic methods [14]. Correlated disorder is known to play an important role in various transport phenomena, for both classical [35] and quantum waves [36], and it is thus relevant to investigate if it constitutes a limitation in the implementation of transfers via shortcut to adiabaticity. As one seeks to obtain a perfect population transfer on the single site A_N, the quantum fidelity $\mathcal{F}$ of the protocol corresponds to the transfer probability $p_{A_N} = |\langle A_N|\psi(T)\rangle|^2$.

A. Simplification and resilience to imperfect realization of the protocol in a simple SSH chain

For a SSH chain of $2N-1$ atoms, our transfer procedure involves the accurate control of $N-1$ couplings associated to NNN interactions with distinct time dependence. From this respect, the accurate implementation of these different couplings, such as those shown in Fig. 3, seems challenging experimentally. To partially overcome this limitation, we suggest here an alternative and simpler implementation. Figure 3 reveals that the shape of the couplings $\rho_n(t)$ to be engineered essentially varies near the edges of the chain. Indeed, if the index n corresponds to atoms near the middle of the chain, the values of the NNN couplings $\rho_n(t)$, $\rho_{n+1}(t)$ and $\rho_{n-1}(t)$ hardly vary. With these considerations in mind, we introduce a simplified approximate protocol where most of the NNN coefficients have a common time-dependent profile. Specifically, we set $\tilde{\rho}_n^{(i)}(t) = \rho_{N/2}(t)$ for $n = i, ..., N-i$, and $\tilde{\rho}_n^{(i)}(t) = \rho_n(t)$ for $n = 1, ..i-1$ and $n = N-i+1, ..N-1$. The NNN couplings $\rho_n(t)$ correspond to the exact NNN transfer protocol. The lower the index i, the simpler the protocol $\tilde{\rho}_k^{(i)}(t)$. The protocol obtained for $i = 1$ involves only a single function for all NNN couplings, while the choice $i = \lceil N/2 \rceil$ amounts to the exact procedure.

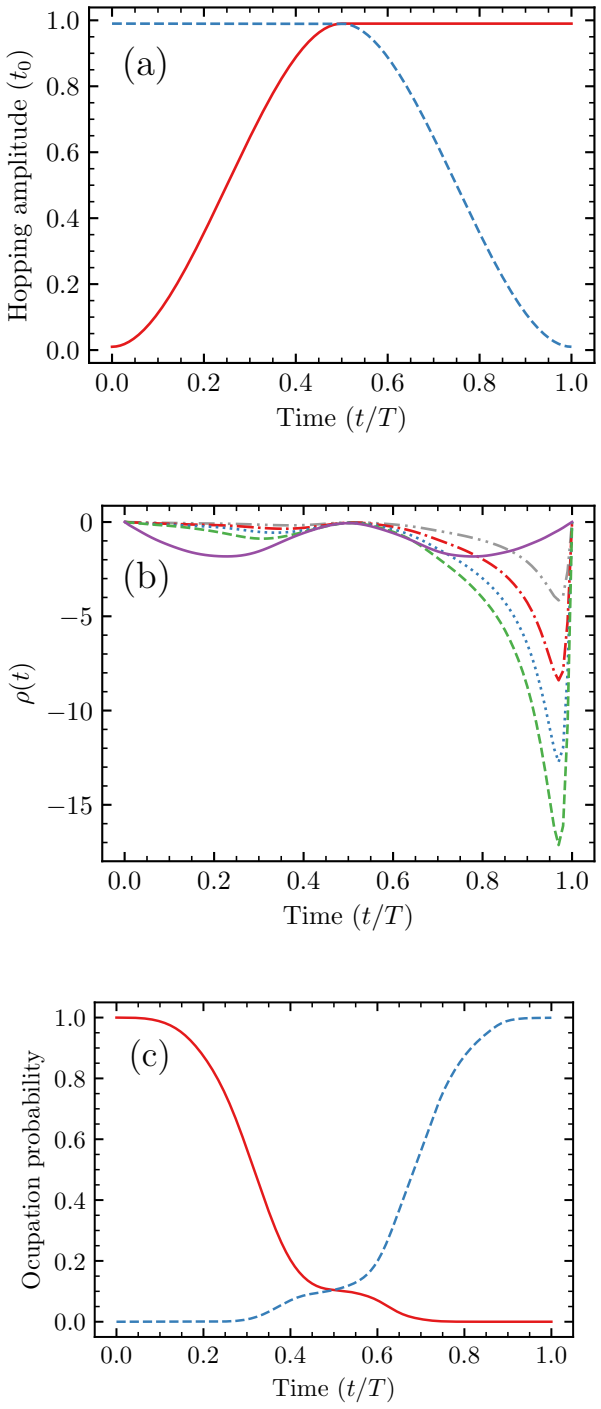

FIG. 5: (a) Hopping amplitudes $t_{2R}(t)$ and $t_{2L}(t)$ as a function of the normalized time t/T (solid blue line and dashed red line respectively). (b) Couplings $\rho_n(t)$ (in units of t_0) for $n = 1, ..., 5$ as a function of time t/T (dash-dot-dotted gray, dash-dotted red, dotted blue, dashed green and solid purple lines respectively). We have taken $N = 5$, corresponding to a SSH chain of $4N - 1 = 19$ sites, and a total time $T = 40/t_0$. (c) Time-dependent probability of occupation of the sites $|A_1\rangle$ (red line) and $|A_{2N}\rangle$ (dashed blue line) in a SSH chain with topological interface and NNN-assisted transfer protocol. The chain comprises $4N - 1 = 19$ sites, and the total duration is $T = 40/t_0$.

In this alternative implementation, the trade-off between the quality of the quantum state transfer and the simplification brought by the substitution is crucial. Remarkably, values of i of a few units already yield a quantum fidelity close to unity. Table I gives the transfer probability achieved for the approximate protocol $\tilde{\rho}_n^{(i)}(t)$ in a chain with $N = 10$ sites in sublattice A and for several approximation levels i, demonstrating the fast convergence of the method.

TABLE I: Transfer probability $p_{A_{10}}$ versus index i for the simplified NNN protocol in a single SSH chain (Fig. 1). The index i measures the approximation degree of the exact NNN protocol.

i	1	2	3	4
$p_{A_{10}}$	0.12	0.88	0.87	0.99

We now discuss the robustness of our protocol against stochastic fluctuations of the counter-diabating driving terms. For this purpose, we consider a noisy realization of the complete protocol (i.e. without the approximation proposed in the previous section), where the NNN couplings now correspond to stochastic variables $\hat{\rho}_n(t)$. We introduce a random variable $G(\delta E)$, following a centered Gaussian distribution (i.e. null expectation value) with unit standard deviation and area δE, and set $\hat{\rho}_n = (1 + G(\delta E))\rho_n(t)$. The form of the profiles is preserved, but these are multiplied by a stochastic factor, which could be related for instance to a large-scale fluctuation of a control laser field. Figure 6 shows the results obtained for 10^4 disorder realizations. The numerical simulations indicate that the quantum state transfer is achieved with a fidelity $\mathcal{F}$ above 95% for almost all the realizations despite the presence of significant fluctuations in the amplitude of the NNN interactions (error of the order of 20%). Most of the realizations show indeed a transfer probability above 98%.

B. Robustness of the NNN protocol against uncorrelated disorder in the SSH chain

We discuss here the resilience of the protocol against fluctuations in the eigenenergies of the SSH Hamiltonian. Let us consider first the SSH chain of Fig. 1 without interface. Precisely, we assume that the Hamiltonian can be written as $H'(t) = H(t) + \delta H$ with a stochastic contribution $\delta H = t_0\,\mathrm{Diag}[G(\delta E)]$ corresponding to a diagonal matrix whose elements are static, statistically independent random variables following a Gaussian distribution $G(\delta E)$ centred around zero with an area δE and unit standard deviation. Figure 7a compares the behavior of the NNN-interaction protocol with the adiabatic Landau-Zener (LZ) protocol of Ref. [14] for the same amount of disorder in the eigenenergies. For convenience, we recall here the form of the LZ protocol that can be implemented

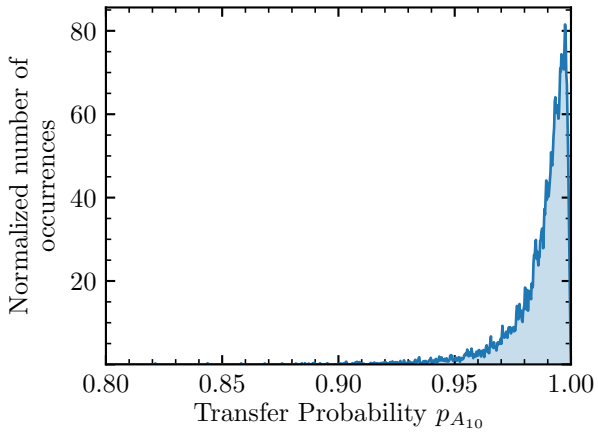

FIG. 6: Normalized distribution of the transfer probability $p_{A_N} = |\langle A_N|\psi(T)\rangle|^2$ obtained from 10.000 realizations of the NNN protocol in a single SSH chain (see Fig. 1), with a common stochastic bias factor multiplying the NNN couplings $\rho_n(t)$. The stochastic factor is centered on 1 and has a Gaussian distribution of standard deviation $\sigma = 1$ and area $\delta E = 0.2$. The NN hopping amplitudes, the total duration and the error-free NNN couplings $\rho_n(t)$ are identical to Fig. 2.

using a Rice-Mele Hamiltonian:

$$t_1(t) = t_0$$

$$t_2(t) = \begin{cases} t_0 \frac{1-\epsilon}{2}[1-\cos(\pi t/\tau)] & 0 < t < \tau \\ t_0(1-\epsilon) & \tau < t < \tau + \tau_z \\ t_0 \frac{1-\epsilon}{2}[1-\cos(\pi(t-\tau_z)/\tau)] & \tau + \tau_z < t < T \end{cases} \quad (13)$$

$$\delta(t) = \begin{cases} \delta_0 & 0 < t < \tau \\ \delta_0 - \alpha(t-\tau)/2 & \tau < t < \tau + \tau_z \\ -\delta_0 & \tau + \tau_z < t < T. \end{cases}$$

In the above equations, $\delta(t)$ is the time-dependent energy difference between the A and B sites, which realizes a linear ramp during the duration τ_z. The total time is $T = 2\tau + \tau_z$, and $\alpha = 4\delta_0/\tau_z$.

In contrast to the LZ protocol, for which the distribution extends to 92%, the distribution of transfer probability p_{A_N} associated to the NNN protocol stays above 97.5% for almost all realizations. This is a remarkable and rather unexpected result, as the Landau-Zener transition belongs to the class of adiabatic protocols, which as such is expected to have a stronger resilience than our NNN-interaction protocol.

We have done a similar investigation in a SSH chain with a topological interface. In order to ease the comparison with the transfer in a single SSH chain, we have taken an identical total duration $T = 2/t_0$. Our results, depicted in Fig. 7(b), show that the transfer probability remains above 98% for most of the realizations when submitted to the same uncorrelated disorder as previously. The presence of a topological interface in the SSH chain slightly reduces the resilience of the NNN protocol, but its robustness in this context is still impressive.

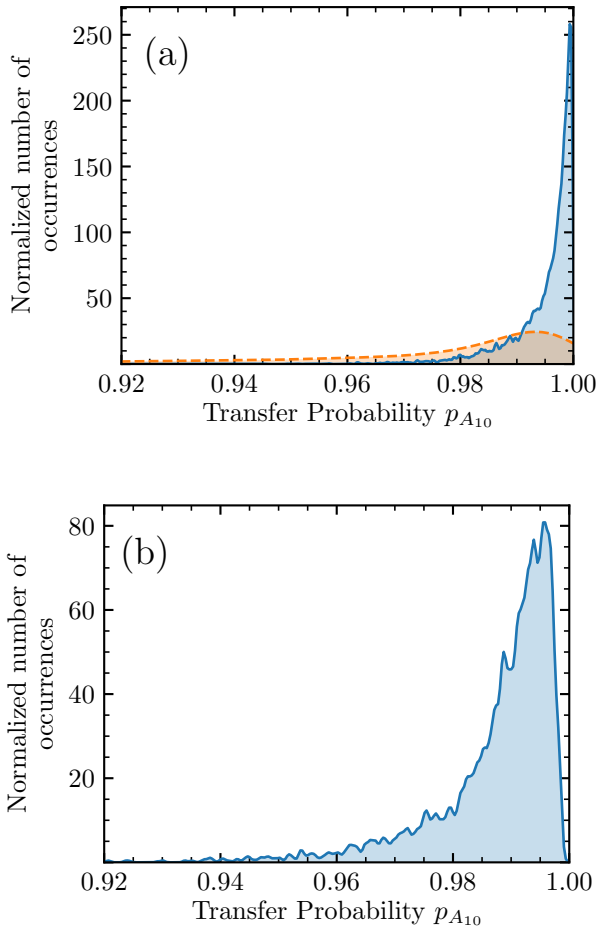

FIG. 7: Normalized distribution of the transfer probability $p_{a_{2N}}$ for the nonadiabatic NNN protocol (a) in a simple SSH chain (solid blue lines) along with the distribution associated to the adiabatic LZ protocol (dashed orange line) and (b) in a SSH chain with topological interface (solid blue lines). Diagonal terms of the Hamiltonian are subjected to an uncorrelated Gaussian disorder $\delta E = t_0 G(\alpha)$ with $\alpha = 0.2$. We have used 10.000 realizations for the NNN protocol in (a), and 5000 for the LZ protocol and NNN protocol in (b). Parameters of the NNN protocol in (a) are identical to Fig 2. Parameters for the LZ protocol are the same to those of Fig. 3 in Ref. [14] except for the chain size ($N = 9$) and for the transfer time ($T = 220/t_0$). The NNN protocol in the SSH chain with topological interface (b) is identical to Fig. 5, except for the transfer time ($T = 2/t_0$).

In order to obtain a more quantitative picture of the robustness of the NNN protocol, we investigate the standard deviation of the quantum fidelity versus the disorder amplitude δE. Figure 8 shows the standard deviation of the transfer probability p_{A_N} obtained in the LZ and NNN protocols for different amount of disorder. The results clearly indicate that the NNN protocol is more

resilient for the considered range of disorder amplitudes. As expected, the standard deviation increases with the strength of disorder. Even if we consider the combined effects of uncorrelated disorder in both the eigenenergies and in the couplings ρ_n for the NNN transfer method, it outperforms the LZ protocol, as shown in Fig.8.

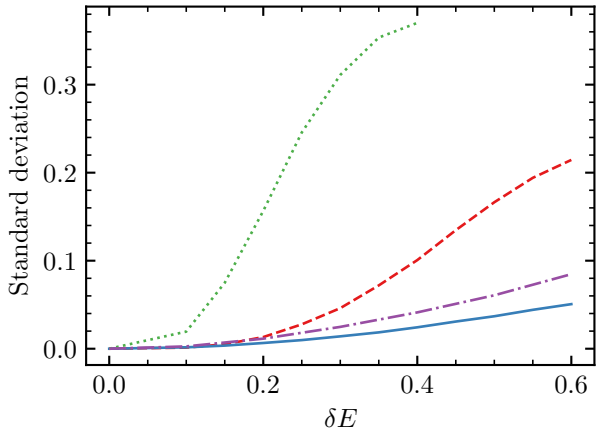

FIG. 8: Standard deviation of the transfer probability distribution for the NNN (solid blue line) and LZ (dotted green line) protocols in a simple SSH chain, and for the NNN protocol in a SSH chain with topological interface (dash-dotted purple line) as a function of the uncorrelated disorder strength δE. The uncorrelated disorder is identical to Fig.7. The dashed red line represents the standard deviation associated to a stochastic factor in the realization of the NNN protocol in a single SSH chain (parameters identical to Fig. 6).

C. Robustness against correlated disorder

In addition to uncorrelated Gaussian disorder, we also investigated the influence of correlated disorder of on-site energies (diagonal disorder) on the fidelity of the transfer protocols for the SSH chain. More precisely, we considered the following power-law correlation [37]

$$\delta E_n = \sum_{k=1}^{N} \frac{\alpha}{k^{\gamma/2}} \cos\left(\frac{4\pi n k}{2N-1} + \phi_k\right) \qquad (14)$$

where N is the number of sites in sublattice A, ϕ_k is a random phase and γ is a parameter that sets the correlation length. $\gamma = 0$ corresponds to an uncorrelated disorder while $\gamma > 0$ accounts for a disorder with a long-range correlation in the chain. The correlation length is an increasing function of this exponent.

We have investigated the influence these correlations in protocols applied in both the single SSH chain and in the double SSH chain with a topological interface. Typical numerical results are shown in Fig. 9. For both kind of chains, the standard deviation of the transfer probability decreases with the degree of correlation as better performance are obtained for higher values of the exponent γ. We conclude that these protocols are more robust against correlated disorder than against uncorrelated Gaussian disorder. The presence of correlations indeed mitigates the influence of the disorder on the performance of the NNN transfer protocols. This finding unveils how disorder, and in particular the emerging concept of disorder engineering by introducing correlations [35], may not only degrade but also be used to control transfer protocols.

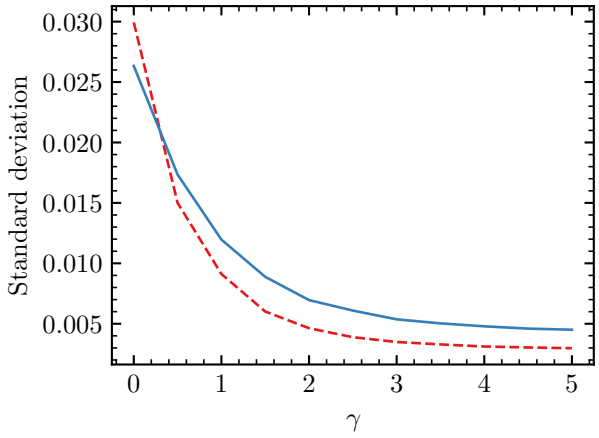

FIG. 9: Standard deviation of the occupation probability p_{a10} at the right boundary as a function of the exponent γ for the NNN protocol in a single SSH chain (solid blue line) and in a double SSH chain with a topological interface (dashed red line). We have taken a diagonal correlated disorder following the power law (14) with $\alpha = 0.2$, a transfer time $T = 2/t_0$, and averaged over 10^4 realizations.

V. CONCLUSIONS AND PERSPECTIVES

Summing up, we have presented an excitation transfer protocol in SSH chains based on a fast evolution of a topological eigenstate, balanced by a counterdiabatic driving through a dynamical control of NNN interactions. The hopping terms are dynamically controlled in the spirit of current experimental platforms for SSH chains [29]. A simplified scheme has been proposed to use a common control field in a large part of the chain. This protocol, which rests on a dynamical control of NN and NNN interactions, shows a strong resilience against fluctuations in the amplitude of the control field and against uncorrelated disorder in the eigenenergies of the SSH Hamiltonian. Interestingly, the method can be extended to realize fast and robust excitation transfer even in SSH chains displaying two segments of different topologies. This result constitutes, to our knowledge, the first example of shortcut-to-adiabaticity protocol involving the crossing of a topological interface. The robustness of the

fast protocol against disorder outperforms even adiabatic methods such as the Landau-Zener or STIRAP protocols. Finally, we have found that the presence of correlation in the disorder mitigates the degradation of the fidelity of the quantum state transfer, indicating that judicious engineering of correlated disorder could enhance the efficiency of the transfer protocols in topological chains.

VI. ACKNOWLEDGMENTS

This work is part of the INCT-IQ from CNPq. F.M.D.A., F.A.P. and F.I. acknowledge support from the agencies CNPq (Grants Universal Faixa B No. 403366/20160 and No. 409994/2018-9), CAPES, and FAPERJ. This work is also funded by the Agence Nationale de la Recherche through Grant No. ANR-18-CE30-0013 (D.G.-O.).

[1] D. Bacon, J. Kempe, D. A. Lidar, and K. B. Whaley Phys. Rev. Lett. 85, 1758 (2000).
[2] A. Y. Kitaev, Physics Uspekhi **44**, 131 (2001).
[3] N. Lang and H. P. Büchler, npj Quantum Information, **3**, 47 (2017).
[4] Y. E. Kraus, Y. Lahini, Z. Ringel, M. Verbin, and O. Zilberberg, Phys. Rev. Lett. **109**, 106402 (2012).
[5] R.J. Chapman, M. Santandrea, Z. Huang, G. Corrielli, A. Crespi, M.-H. Yung, R. Osellame, and A. Peruzzo, Nature Commun. **7**, 11339 (2016).
[6] P. St-Jean, V. Goblot, E. Galopin, A. Lemaître, T. Ozawa, L. Le Gratiet, I. Sagnes, J. Bloch, and A. Amo, Nature Photon. **11**, 651 (2017).
[7] A. Blanco-Redondo, B. Bell, D. Oren, B.J. Eggleton, and M. Segev, Science **362**, 568 (2018).
[8] S. de Léséleuc, V. Lienhard, P. Scholl, D. Barredo, S. Weber, N. Lang, H.P. Büchler, T. Lahaye, and A. Browaeys, Science **365**, 775 (2019).
[9] W. P. Su, J. R. Schrieffer, and A. J. Heeger, Phys. Rev. Lett. **42**, 1698 (1979).
[10] G. M. Nikolopoulos, D. Petrosyan, and P. Lambropoulos, Europhys. Lett. **65**, 297 (2004).
[11] S. Paganelli, S. Lorenzo, T. J. G. Apollaro, F. Plastina, and G. L. Giorgi, Phys. Rev. A **87**, 062309 (2013).
[12] M. P. Estarellas, I. D' Amico, and T. P. Spiller, Sci. Rep. **7**, 42904 (2017).
[13] M. Bello, C. E. Creffield, and G. Platero, Sci. Rep. **6**, 22562 (2016).
[14] S. Longhi, G. L. Giorgi, and R. Zambrini, Adv. Quantum Technol. **2**, 1800090 (2019).
[15] S. Longhi, Phys. Rev. B **99**, 155150 (2019).
[16] D. Guéry-Odelin, A. Ruschhaupt, A. Kiely, E. Torrontegui, S. Martínez-Garaot, and J. G. Muga, Rev. Mod. Phys. **91**, 045001 (2019).
[17] A. Baksic, R. Belyansky, H. Ribeiro, and A.A. Clerk, Phys Rev A **96**, 021801(R) (2017).
[18] X. Shi, H. Yuan, X. Mao, Y. Ma, and H. Q. Zhao, Phys. Rev. A **95**, 052332 (2017).
[19] R. R. Agundez, C. D. Hill, L. C. L. Hollenberg, S. Rogge, and M. Blaauboer Phys. Rev. A **95**, 012317 (2017).
[20] B.-H. Huang, Y.-H. Kang, Y.-H. Chen, Z.-C. Shi, J. Song, and Y. Xia, Phys. Rev. A **97**, 012333 (2018).
[21] H. Zhou, X. Chen, X. Nie, J. Bian, Y. Ji, Z. Li, and X. Peng, Sci. Bull. **64**, 888 (2019).
[22] I. Brouzos, I. Kiorpelidis, F. K. Diakonos, and G. Theocharis, arXiv:1911.03375 (2019).
[23] N.V. Vitanov, arXiv:2004.08341 (2020).
[24] H. Zhou, Y. Ji, X. Nie, X. Yang, X. Chen, J. Bian, and X. Peng, Phys. Rev. Applied **13**, 044059 (2020).
[25] E.J. Meier, K. Ngan, D. Sels, and B. Gadway, e-print arXiv:2005.07052 (2020).
[26] F. Mei, G. Chen, L. Tian, S.-L. Zhu, and S. Jia, Phys. Rev. A **98**, 012331 (2018).
[27] R. Chaunsali, E. Kim, A. Thakkar, P. G. Kevrekidis, and J. Yang. Phys. Rev. Lett. **119**, 024301 (2017).
[28] M. Atala, M. Aidelsburger, J. T. Barreiro, D. Abanin, T. Kitagawa, E. Demler, I. Bloch, Nature Phys. **9**, 795 (2013).
[29] E. J. Meier, F. Alex An and B. Gadway, Nature Comm. **7**, 13986 (2016).
[30] M. V. Berry, J. Phys. A:Math. Theor **42**, 365303 (2009).
[31] Xi Chen, I. Lizuain, A. Ruschhaupt, D. Guéry-Odelin, and J. G. Muga, Phys. Rev. Lett. **105**, 123003 (2010).
[32] Qi Zhang, Xi Chen and D. Guéry-Odelin , Sci. Rep. **7**, 15814 (2017).
[33] F. Impens and D. Guéry-Odelin, Phys. Rev. A **96**, 043609 (2017).
[34] F. Impens, R. Duboscq, and D. Guéry-Odelin, e-print arXiv:2003.05845 (2020).
[35] G. M. Conley, M. Burresi, F. Pratesi, K. Vynck, and D. S. Wiersma Phys. Rev. Lett. **112**, 143901 (2014).
[36] Q. Li, E. H. Hwang, E. Rossi, and S. Das Sarma, Phys. Rev. Lett. **107**, 156601 (2011).
[37] G. Almeida, C. Mendes, M. Lyra, and F. Moura, Ann. Phys. **398**, 180 (2018).